Thursday, 14 March 1985

Chairmen: R.E. Diebold
F. Takasaki
S. Ozaki
J.-M. Gaillard

W and Z Bosons

W and Z Properties in the Electron Channel

Presented by J. Sass, Saclay

No written contributuion received.

W AND Z PRODUCTION PROPERTIES AT THE CERN SPS COLLIDER

UA1 Collaboration, CERN, Geneva, Switzerland

Aachen - Amsterdam (NIKHEF) - Annecy (LAPP) - Birmingham - CERN - Harvard - Helsinki - Kiel - London (Queen Mary College) - Paris (Coll. de France) - Riverside - Rome - Rutherford Appleton Lab. - Saclay (CEN)- Vienna - Wisconsin Collaboration

(Presented by S. Geer)

ABSTRACT

The production properties of Intermediate Vector Bosons produced at the CERN Super Proton Synchrotron (SPS) Collider are described. The longitudinal and transverse momentum distributions, and the properties of the hadronic jet activity produced in association with the Intermediate Vector Bosons, are in impressive agreement with the expectations of the QCD improved Drell–Yan mechanism.

1. Introduction

Data taken at the CERN SPS $\bar{p}p$ Collider during 1982 and 1983 have firmly established the existence of the charged ($W^{\pm}$) and neutral (Z^0) Intermediate Vector Bosons (IVBs) [1]. During this period the UA1 experiment [2] collected essentially background-free samples of 68 $W^{\pm} \rightarrow e^{\pm}\nu_e$ decays [3], 14 $W^{\pm} \rightarrow \mu^{\pm}\nu_{\mu}$ decays [4], 4 $Z^0 \rightarrow e^+e^-$ decays [5], and 5 $Z^0 \rightarrow \mu^+\mu^-$ decays [6]. The production properties of these IVBs were shown to be in good agreement with QCD expectations [7, 8], with the exception of an apparent excess of jet activity produced in association with the neutral Intermediate Vector Bosons. It was concluded, however, that more data were required in order to decide whether this excess of jet activity was due to a statistical fluctuation, or to new and unexpected physics.

The recent 1984 data-taking period has enabled the UA1 Collaboration to triple the size of its IVB event samples, yielding a total of 201 $W^{\pm} \rightarrow e^{\pm}\nu_e$ decays, and 31 $Z^0 \rightarrow \ell^+\ell^-$ decays ($\ell^+\ell^- = e^+e^-$ or $\mu^+\mu^-$). These larger event samples enable a more detailed measurement of the production properties to be made. Preliminary results on the measurement of the longitudinal and transverse momentum distributions of the IVBs, and on the properties of hadronic jets produced in association with the IVBs, are presented in this paper, which is organized as follows. In Section 2 the longitudinal momentum distributions of the IVBs are discussed. The data are shown to be in agreement with our naïve expectations for Drell-Yan production of $W^{\pm}$'s and Z^0's. In Section 3 the transverse momentum distribution of the W's and the jet activity produced in association with the W's are shown to be in good agreement with the expectations of QCD perturbation theory. There is, however, a need for more detailed higher-order calculations to be made. The corresponding properties for Z^0 production are shown to be consistent with those of the W. This includes the jet activity produced in association with the Z^0. Finally, in Section 4 some conclusions are presented.

2. Longitudinal Momentum

Consider first the longitudinal momentum distribution of W's extracted from the $W^\pm \to e^\pm \nu_e$ event sample. Unfortunately we do not measure the longitudinal momentum of the W directly since we do not measure the longitudinal component of the neutrino momentum. We can overcome this difficulty by imposing the mass of the W on the electron-neutrino system. This will yield two solutions for the longitudinal component of the neutrino momentum, one corresponding to the neutrino being emitted forwards in the W rest frame, the other corresponding to the neutrino being emitted backwards. Hence we have two solutions for x_W, the Feynman x for the W. In practice, in one-third of the events one of these two solutions for x_W is trivially unphysical ($x_W > 1$), and in another one-third the ambiguity is resolved after consideration of energy and momentum conservation in the whole event [9]. In the cases where the ambiguity in x_W is resolved, it tends to be nearly always the lowest of the two x_W solutions which is chosen. In the following preliminary analysis the lowest of the two solutions will be used for all the events. The bias that this choice introduces will be built into the model used to describe the data.

The x_W distribution is shown in Fig. 1a. We would expect the longitudinal motion of the W to reflect the structure functions of the incoming partons. For comparison with the data we will assume that W production proceeds via the Drell–Yan mechanism involving the annihilation of a u ($\bar{u}$) quark with a $\bar{d}$ (d) antiquark, and use the structure functions of Eichten et al. [10] with $\Lambda = 0.2$ GeV for the incoming partons. In W production these structure functions are sampled at the W pole, i.e.

$$x_u x_d = \tau, \tag{1}$$

where x_u and x_d are the Feynman x for the u- and d-quarks making the W, and

$$\tau = m_W^2/s,$$

where s is the centre-of-mass energy squared and m_W the W mass. To extract x_W we can use momentum conservation

$$x_W = |x_u - x_d| . \tag{2}$$

The bias introduced by always choosing the low x_W solution for the longitudinal component of the neutrino momentum is accounted for with a Monte Carlo program in which experimental resolution is included. The resulting prediction for the x_W distribution gives a good description of the data (Fig. 1a).

We can go further since we can use energy and momentum conservation [Eqs. (1) and (2)] to extract the proton and antiproton quark-distributions sampled by the W. The results are shown in Fig. 2. A comparison of the two distributions provides us with a CP test since valence quarks in the proton should look like valence antiquarks in the antiproton. The two distributions are consistent with each other, and are well described by the Eichten et al. curve. We can go still further for those events in which the charge of the electron (and hence W) is well determined. In this case we can identify the proton quark with a u quark (for a W^+) or a d quark (for a W^-). The resulting u-quark and d-quark x-distributions are shown in Figs. 3 and 4. Once again they are well described by the expectations of Eichten et al.

Now consider the longitudinal momentum distribution of the Z^0's. In this case we measure x_Z directly. The result is shown in Fig. 1b, and is consistent with the corresponding distribution for the W's. The limited Z^0 statistics, however, prevent us from being able to extract the quark distributions in the proton and antiproton with any precision. Clearly when more data become available the Z^0 will offer a cleaner way of extracting these structure functions.

3. Transverse Momentum

IVB production at the CERN $p\bar{p}$ Collider is expected to proceed by the Drell-Yan mechanism in which a quark from the proton annihilates with an antiquark from the antiproton. In a QCD-improved picture of the production mechanism the annihilating quark and antiquark are coloured, and there will be higher-order corrections to the bare Drell-Yan process in which one or more gluons are radiated from the incoming partons. This initial-state gluon bremsstrahlung is expected to give rise to i) a long tail in the transverse momentum distribution of the weak bosons, and ii) the occasional observation of one or more hadronic jets produced in association with the higher transverse momentum IVBs. In the region in which QCD perturbation theory is applicable (for sufficiently large transverse momentum jets), the rate of occurrence of this jet activity is determined by the strong coupling constant α_s. Knowledge of the rate and properties of hadronic jets produced in association with the weak bosons therefore enables us to make a quantitative test of QCD, and in future will hopefully provide us with a measurement of α_s.

3.1 Experimental and theoretical considerations

In practice, analysis of the relatively low transverse energy jets arising from initial state gluon bremsstrahlung is not straightforward. There are a number of experimental and theoretical difficulties which must be overcome:

1) The soft non-perturbative part of the hadronization process which turns the underlying parton into an observable hadronic jet is not at present well understood. Since this process controls the geometrical size, the particle content, and the fragmentation function for the jets, the theoretical uncertainty results in a systematic uncertainty in the experimental reconstruction efficiency for a jet of a given transverse energy. It also results in a systematic uncertainty in the relationship between the reconstructed energy and momentum of the hadronic jet and the four-momentum of the underlying parton. In practice we have used the ISAJET Monte Carlo [11] to study both these problems. This is a very simplistic QCD-inspired Monte Carlo in which the transverse momentum of every W is balanced by one recoiling gluon. The gluon then fragments with the fragmentation function of Field and Feynman [12], and the resulting hadronic jet is reconstructed by employing a sophisticated and fairly complete simulation of the UA1 detector. Using the UA1 jet algorithm and the cuts described below, the reconstruction efficiency for the ISAJET jets arising from initial-state gluons associated with W production is 50%. This reconstruction efficiency has been taken into account when comparing theoretical expectations with the experimental results for the rate of jet activity and the multiplicity distribution of jets in W events. A full study of energy and momentum corrections for these low transverse momentum jets is, however, not yet complete, and so for definiteness no corrections have been applied to the measured jet four-vectors. An initial study of these corrections suggests that the jet energy is systematically underestimated by about 20% and the momentum by about 10%. Although they have not been applied to the data, these corrections have been fully taken into account in the Monte Carlo curves presented in this paper.

2) There is a small loss of the more active $W^{\pm} \rightarrow e^{\pm}\nu_e$ events which arises because we require an isolated electron in defining our data sample. Clearly the electron isolation depends upon the properties

of the underlying event, and is once again not well understood theoretically. However, we have studied the loss of events due to our electron isolation criteria by means of a Monte Carlo technique in which we use real $W^{\pm} \rightarrow e^{\pm}\nu_e$ events, but generate a random (V–A) decay for the produced W, and examine the isolation of the re-defined electron. We find that we lose 3% of the resulting W events. There is a roughly linear correlation between the size of the loss and the W transverse momentum. The loss rises from essentially zero for the lowest transverse momentum W's to about 6% for the highest transverse momentum W's. The size of the correction is therefore small, and has not been taken into account in the following (preliminary) results.

3) Finally, there is a level of arbitrariness in the experimental definition of a jet. We use the standard UA1 jet algorithm and look for jets with a transverse energy in excess of 5 GeV, and with a jet axis within the rapidity window $|\eta| < 2.5$. The UA1 jet algorithm can resolve two jets if they are separated in (η,ϕ)-space by a distance $\Delta R \equiv (\Delta\eta^2 + \Delta\phi^2)^{1/2}$ of more than 1 unit, where $\Delta\phi$, the azimuthal separation of the two jets, is measured in radians. These features of the jet algorithm have been included in the theoretical curves used to make a comparison with the data.

3.2 Results

In spite of these limitations in our theoretical and experimental understanding of low transverse energy jets, it turns out that our QCD expectations for the rate and properties of the jet activity produced in association with IVBs give a remarkably good description of the data, which is summarized in the following paragraphs.

We begin with the transverse momentum distribution for the W's, shown in Fig. 5. It is well described by the QCD prediction of Altarelli et al. [13]. The distribution has a peak at about 4 GeV/c (primarily reflecting the experimental resolution on the measurement of the missing transverse energy in the event) and a long tail extending to almost 40 GeV/c. The event containing the highest transverse momentum W is shown in Fig. 6. The W is seen to be recoiling against a hadronic jet. The jet transverse momentum balances the transverse momentum of the W. This is a general feature of the jet activity observed in the W events, which can be seen in Fig. 7 where the components of the jet transverse momentum vector, parallel and perpendicular to the direction of the W motion in the transverse plane, have been plotted as a function of the W transverse momentum. In Fig. 8 the imbalance between the W and jet transverse momenta is shown, expressed as a fraction of the W transverse momentum ($|p_T^W - p_T^J|/p_T^W$). The curve, which gives a good description of the data, is a Gaussian with a width given by $\sigma = 0.3\ p_T^W$. This agrees with the expected smearing due mainly to the experimental resolution in reconstructing the jet transverse momentum. Thus within the experimental resolution the transverse momentum of the W–jet system is zero, which implies that we have extracted all the relevant parts of the event. The basic features of the observed jet activity produced in association with charged IVBs are described below.

a) The rate of jet activity is summarized in Table 1. In 35% of the sample of 201 $W^{\pm} \rightarrow e^{\pm}\nu_e$ events, a hadronic jet with transverse momentum in excess of 5 GeV is observed. Defining [8] R_W,

$$R_W \equiv \sigma(W + \text{jet})/\sigma(W),$$

we find $R_W = 0.54 \pm 0.06$. The equivalent fraction for the Z^0 events is $R_Z = 0.7 \pm 0.2$, and the ratio of these ratios is $R \equiv R_Z/R_W = 1.3 \pm 0.4\ (\pm 0.1)$, where the second error is an estimate of the systematic error arising from different selection biases for W and Z^0 events. Clearly, with the increase in statistics from the 1984 data the rate of jet activity observed, produced in association with Z^0's, is consistent with the corresponding rate for W production. The fraction of W events containing jet activity is shown in Fig. 9 as a function of the W transverse momentum in the event. Considering the

Table 1

Rate of occurrence of jets in IVB events

Channel	Number of events					Total number of jets
	Total	$\geqslant$ 1 jet	1 jet	2 jets	3 jets	
$W^{\pm} \rightarrow e^{\pm}\nu_e$	201	71	53	12	6	95
$Z^0 \rightarrow e^+e^-$	22	9	4	4	1	15
$Z^0 \rightarrow \mu^+\mu^-$	9	6	4	0	2	10

simplicity of the calculation, the expectation for this distribution from the ISAJET Monte Carlo is in reasonable agreement with the data. Events with a low transverse momentum W rarely contain jet activity, whereas events with a high transverse momentum W (p_T^W > 20 GeV/c) always contain one or more hadronic jets.

b) The multiplicity distributions for the jets associated with W and Z^0 production are shown in Figs. 10a and 10b, respectively. They are consistent with an exponentially falling distribution, and are in agreement with the QCD curve. This curve is based upon the ISAJET result and the assumption [14] that the probability to produce two jets together with the W is the square of the probability to produce one jet. A more rigorous higher-order QCD calculation is clearly desirable.

c) The transverse momentum distribution for the jets is shown in Figs. 11a and 11b for the W and Z^0 events, respectively. The shapes of the tails of these distributions (the region in which we have a good reconstruction efficiency for the jets) are well described by the QCD calculation of Ref. [8]. Restricting ourselves to those W events containing one and only one jet gives the jet transverse momentum distribution shown in Fig. 11c, which is well described by the ISAJET Monte Carlo.

d) The angular distribution of jets reconstructed in W events is strongly peaked in the beam directions. This can be seen in Fig. 12a where the distribution of cos θ^* is shown, θ^* being the angle between the jet and the average beam direction in the rest frame of the W and the jet. The shape of this distribution is in agreement with the QCD expectation for bremsstrahlung jets of Ref. [8], which is basically $(1 - |\cos\theta^*|)^{-1}$.The corresponding angular distribution for jets in Z^0 events is similar (Fig. 12b).

e) Before we can conclude that the jet activity observed in W events is well understood in the framework of QCD, we must look at the (W + jet)-mass distribution (Fig. 13a) to see if there is any evidence for the production of a state X which subsequently decays into a W and a hadronic jet. There is no clear evidence for such a process. Indeed the prediction from the ISAJET Monte Carlo, which uses the structure function of Eichten et al. [10] with Λ = 0.2 GeV, gives a good description of this mass distribution. Futhermore, if we use event mixing in which the W four-vectors from our sample of 201 $W \rightarrow e^{\pm}\nu_e$ events are associated randomly with the jet four-vectors from the sample of jets reconstructed in these events, the resulting (W + jet)-mass distribution is similar to the ISAJET prediction, and also describes the data. Unfortunately no QCD curves are yet available for the (W + 2 jet)-mass distribution (Fig. 13b) or the (W + 3 jet)-mass distribution (Fig. 13c). However, we can use the event-mixing technique to generate expectations for these distributions. The resulting curves give a satisfactory description of the data. Finally, to be really sure that there is no evidence in the data for the process X $\rightarrow$ (W + jet), we show in Fig. 14 the two-dimensional plot of $|\cos \theta^*|$ versus (W + jet) mass. The population in this plot is well described by the ISAJET expectation. There is no evidence for an excess of central jets anywhere in the [(W + jet) mass, $|\cos \theta^*|$]-plane.

4. Summary and Conclusions

The production properties of $W^\pm$ and Z^0 bosons produced at the CERN SPS $p\bar{p}$ Collider are in agreement with the expectations for IVBs produced by the QCD-improved Drell–Yan mechanism:

i) The longitudinal momentum distributions of the partons participating in W production are in agreement with our expectation using the structure functions of Eichten et al. [10].

ii) The transverse momentum distribution is in agreement with current QCD expectations.

iii) Hadronic jet activity is observed to be produced in association with the higher transverse momentum W's, which is understood in the framework of QCD radiative corrections to the bare Drell–Yan mechanism.

iv) The rate, the transverse-momentum distribution, and the angular distribution for these hadronic jets are in agreement with QCD expectations.

v) There is no evidence for the production of a state X which subsequently decays into W + jet(s).

vi) The production properties for the Z^0's are consistent with the corresponding properties for the W's.

Finally, it is worth noting that in the coming year a further data-taking period is expected, potentially doubling the existing IVB data samples. With this increase in statistics, and with the expected improvement in the experimental understanding of the reconstruction and measurement of low transverse energy hadronic jets, the production properties of the IVBs produced at the Collider should provide us with a demanding quantitative test of QCD, and with a method of determining α_s. At present the main limitations to achieving these goals seem to be theoretical in nature, rather than experimental. In particular there is a clear need for higher-order perturbative QCD calculations [$O(\alpha_s^4)$] including diagrams with virtual corrections etc. In addition, an improvement in understanding the soft non-perturbative hadronization process will help in understanding the relationship between the properties of the underlying parton and the experimental measurement of the properties of the resulting hadronic jet. In spite of these limitations, the current agreement between experiment and QCD expectations is impressive.

REFERENCES

[1] C. Rubbia, Experimental Observation of the Intermediate Vector Bosons W^+, W^-, and Z^0, to be published in 'Les Prix Nobel en 1984'.

[2] UA1 proposal, A 4π solid-angle detector for the SPS used as a proton–antiproton collider at a centre-of-mass energy of 540 GeV, CERN/SPSC 78-06 (1978).

[3] G. Arnison et al. (UA1 Collaboration), Phys. Lett. **122B,** 103 (1983).
G. Arnison et al. (UA1 Collaboration), Phys. Lett. **129B,** 273 (1983).
C. Rubbia, Proc. 4th Topical Workshop on Proton–Antiproton Collider Physics, Berne, 1984 (CERN 84-09, Geneva, 1984), p. 218.

[4] G. Arnison et al. (UA1 Collaboration), Phys. Lett. **134B,** 469 (1984).

[5] G. Arnison et al. (UA1 Collaboration), Phys. Lett. **126B,** 398 (1983).

[6] G. Arnison et al. (UA1 Collaboration), Phys. Lett. **147B,** 241 (1984).

[7] S. Geer, Hadronic jet activity associated with Intermediate Vector Boson production at the SPS Collider, Talk given at the 19th Rencontre de Moriond, La Plagne, 1984.
S. Geer, UA1 results on jet activity associated with $W^\pm$ and Z^0 production at the CERN Proton–Antiproton Collider, preprint CERN-EP/84-160 (1984), talk given at the DPF Annual Meeting, Santa Fe, NM, 1984.

[8] S. Geer and W.J. Stirling, Phys. Lett. **152B,** 373 (1985).

[9] S. Geer, Resolving the x_W ambiguity, internal note UA1/TN 83-45 (1983).

[10] E. Eichten et al., Rev. Mod. Phys. **56,** 579 (1984).

[11] F.E. Paige and S.D. Protopopescu, ISAJET program, BNL 29777 (1981).

[12] R.D. Field and R.P. Feynman, Nucl. Phys. **B136,** 1 (1978).

[13] G. Altarelli et al., Vector boson production at present and future colliders, CERN preprint TH.4015/84 (1984).

[14] S.D. Ellis, R. Kleiss and W.J. Stirling, CERN-TH 4096/85 (1985).

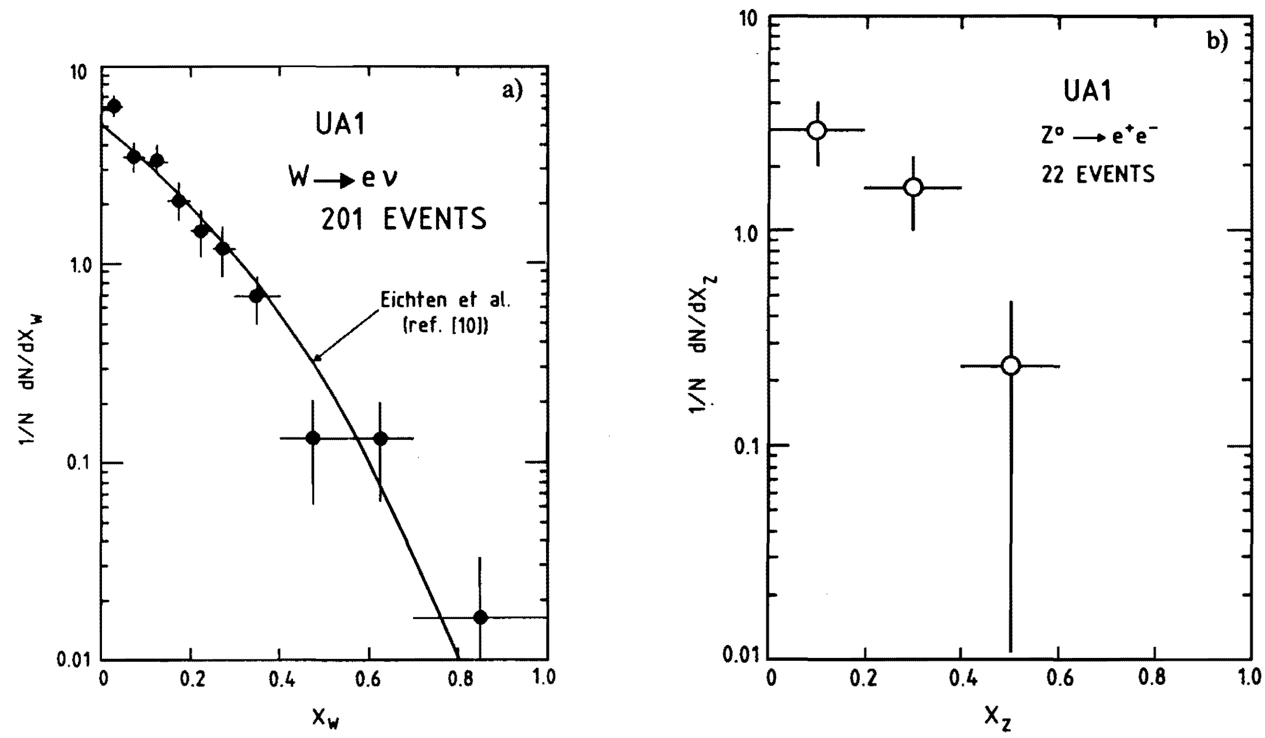

Fig. 1 Longitudinal momentum distribution for IVBs. a) Feynman x-distribution for W's. The curve is the prediction using the model described in the text. b) Feyman x-distribution for Z^0's.

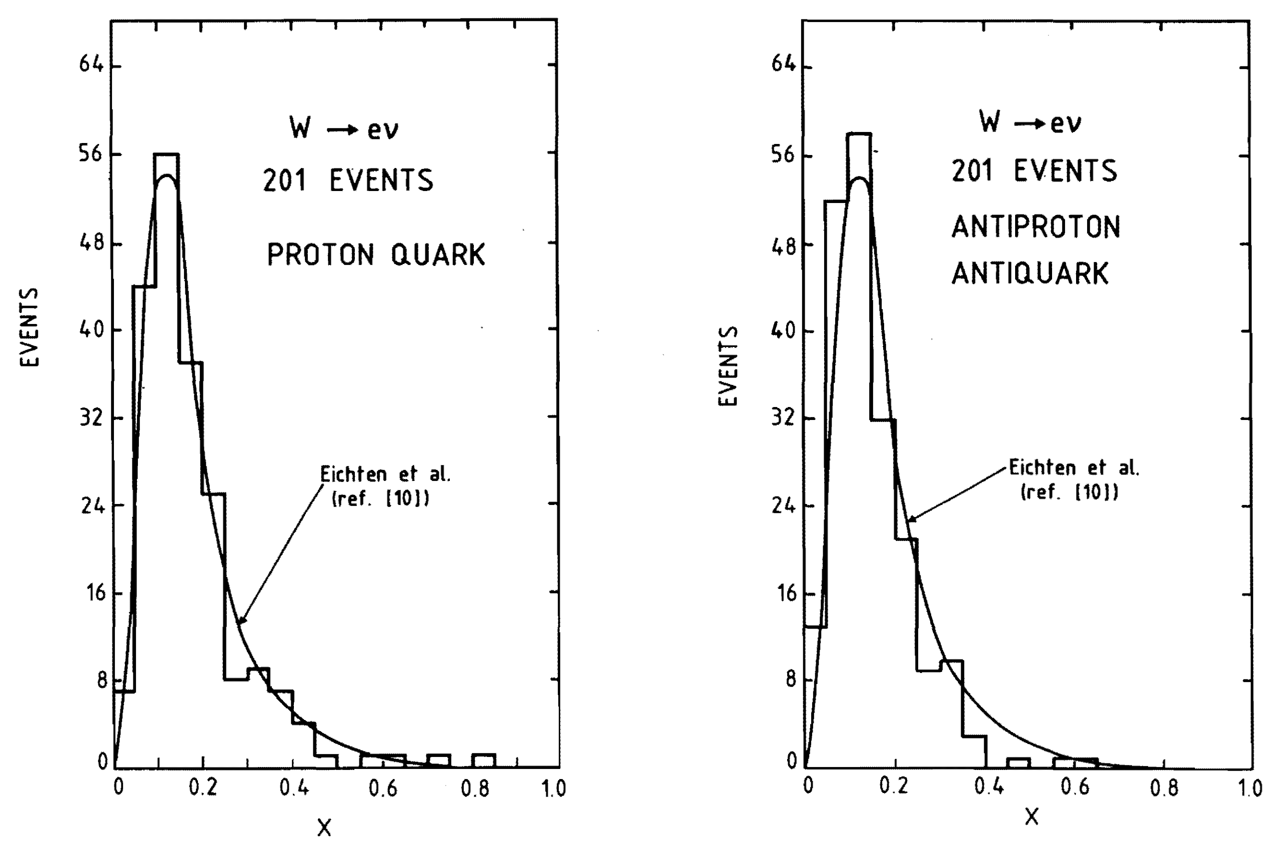

Fig. 2 Proton and antiproton structure functions for those partons producing the W. The curves are the prediction of the model described in the text using the structure functions of Eichten et al. [10] with Λ = 0.2 GeV.

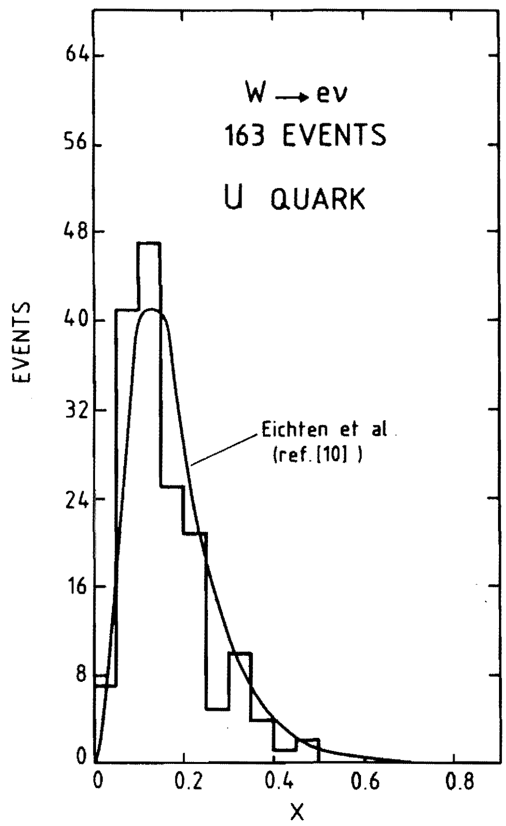

Fig. 3 The u-quark structure function for those u-quarks producing the W. The curve is the prediction of the model described in the text.

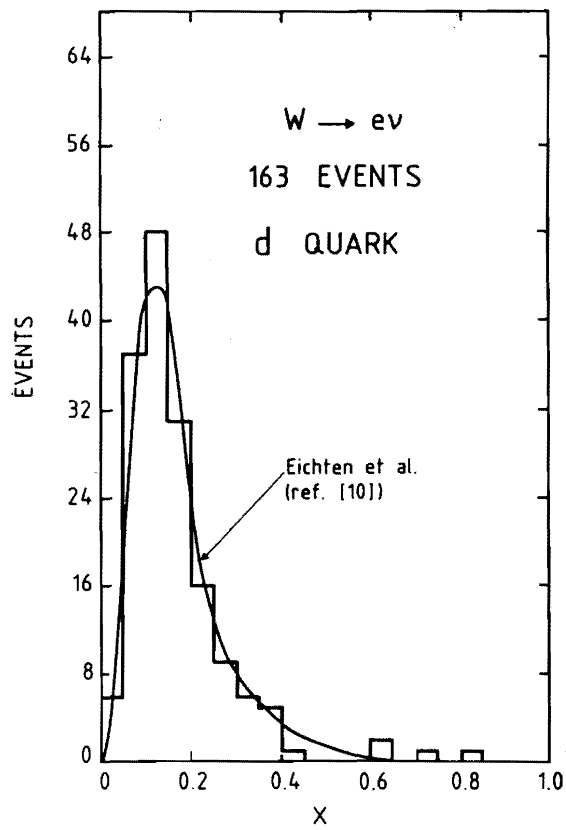

Fig. 4 The d-quark structure funtion for those d-quarks producing the W. The curve is the prediction of the model described in the text.

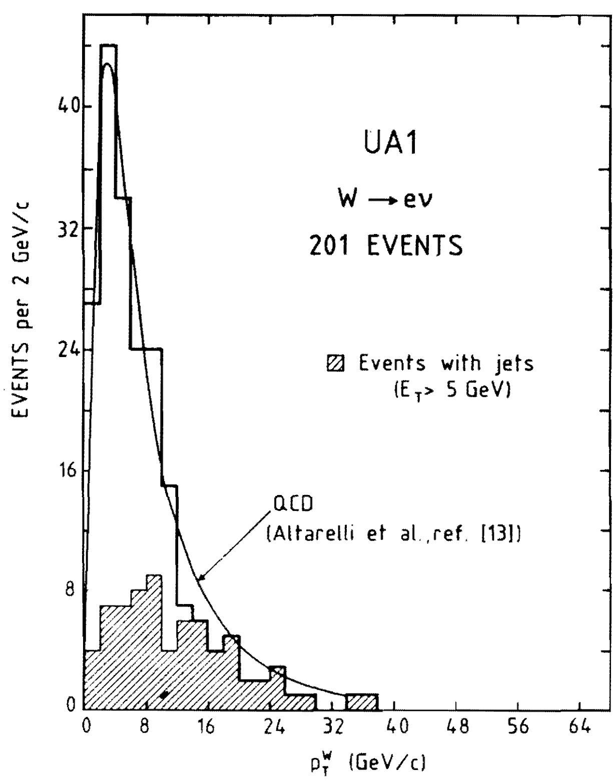

Fig. 5
Transverse momentum distribution for the W. The curve shows the QCD prediction of Altarelli et al. [13]. The shaded sub-histogram shows the contribution from events in which the UA1 jet algorithm reconstructs one or more hadronic jets with transverse momentum in excess of 5 GeV/c in the rapidity interval $|\eta| < 2.5$.

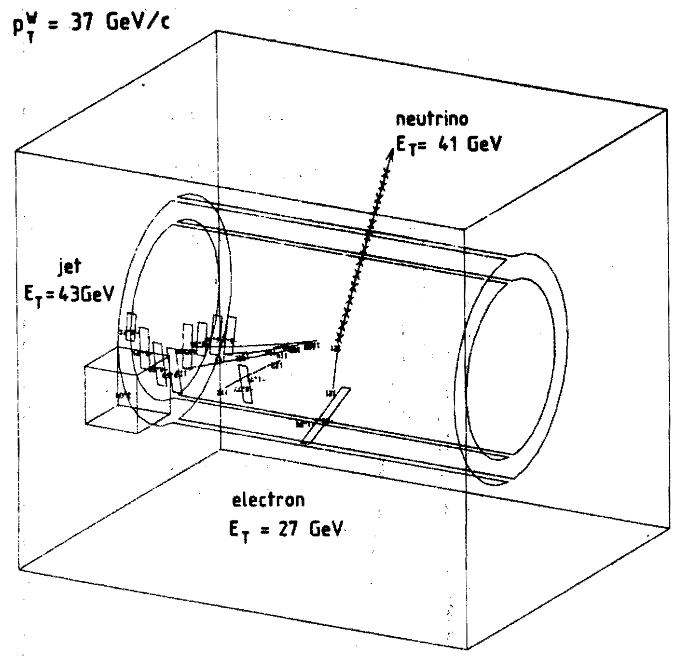

Fig. 6
A graphic display of the UA1 event containing the highest transverse momentum W^- decaying in the $e^- \nu_e$ channel, observed in the 1984 data-taking period. A hadronic jet is seen recoiling against the $(e^- \nu_e)$ system.

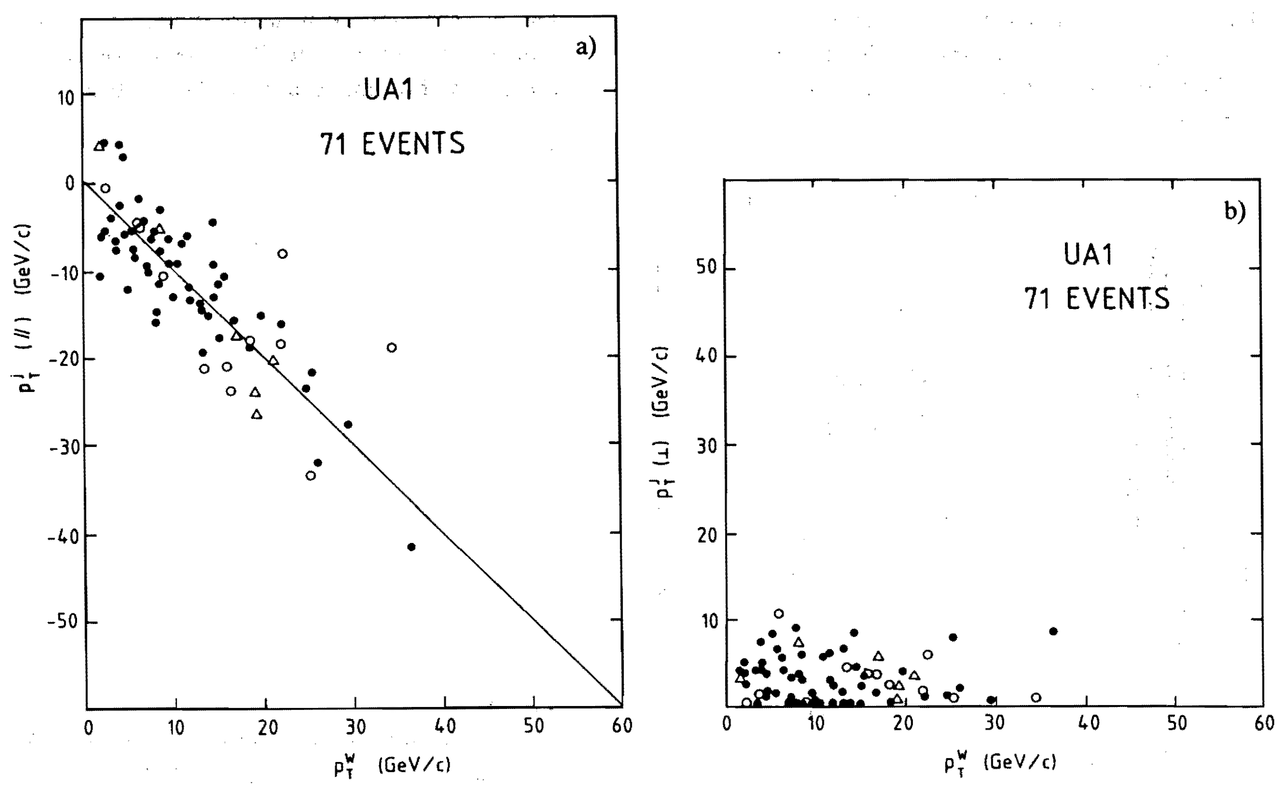

Fig. 7 The hadronic jets, produced in association with W's, recoil against the W in the transverse plane and balance the transverse momentum of the W. a) The component of the jet transverse momentum in the direction of the W transverse momentum vector shown as a function of the W transverse momentum. For events containing two jets (open circles) or three jets (triangles) the vector sum of the jet transverse momenta has been used. b) The component of the jet transverse momentum perpendicular to the direction of the W transverse momentum vector.

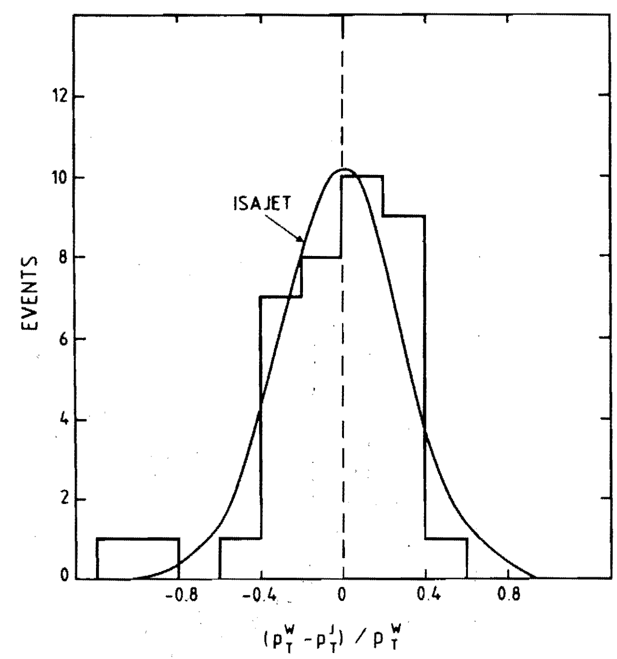

Fig. 8 The jet transverse momentum balances the W transverse momentum. The imbalance between the W and jet transverse momenta is shown as a fraction of the W transverse momentum. The curve is a Gaussian with a width given by $\sigma = 0.3$, reflecting the expected experimental resolution.

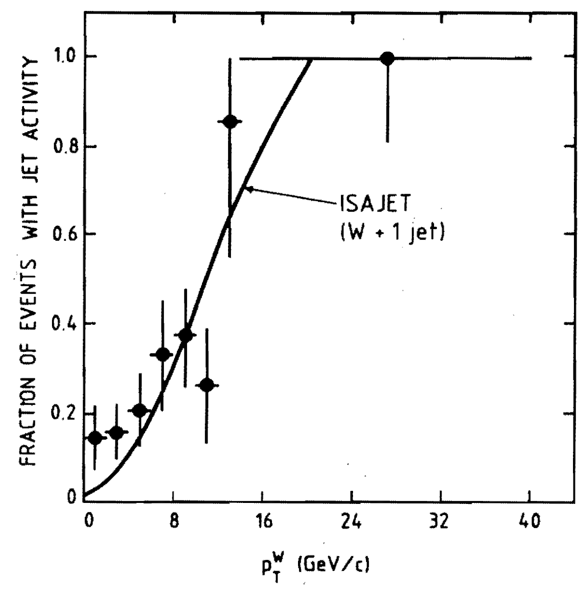

Fig. 9 Jet reconstruction efficiency. The fraction of W events in which hadronic jet activity is observed is shown as a function of the W transverse momentum. The curve is the ISAJET prediction for this distribution, which for ISAJET is simply the jet reconstruction efficiency shown as a function of the underlying parton transverse momentum.

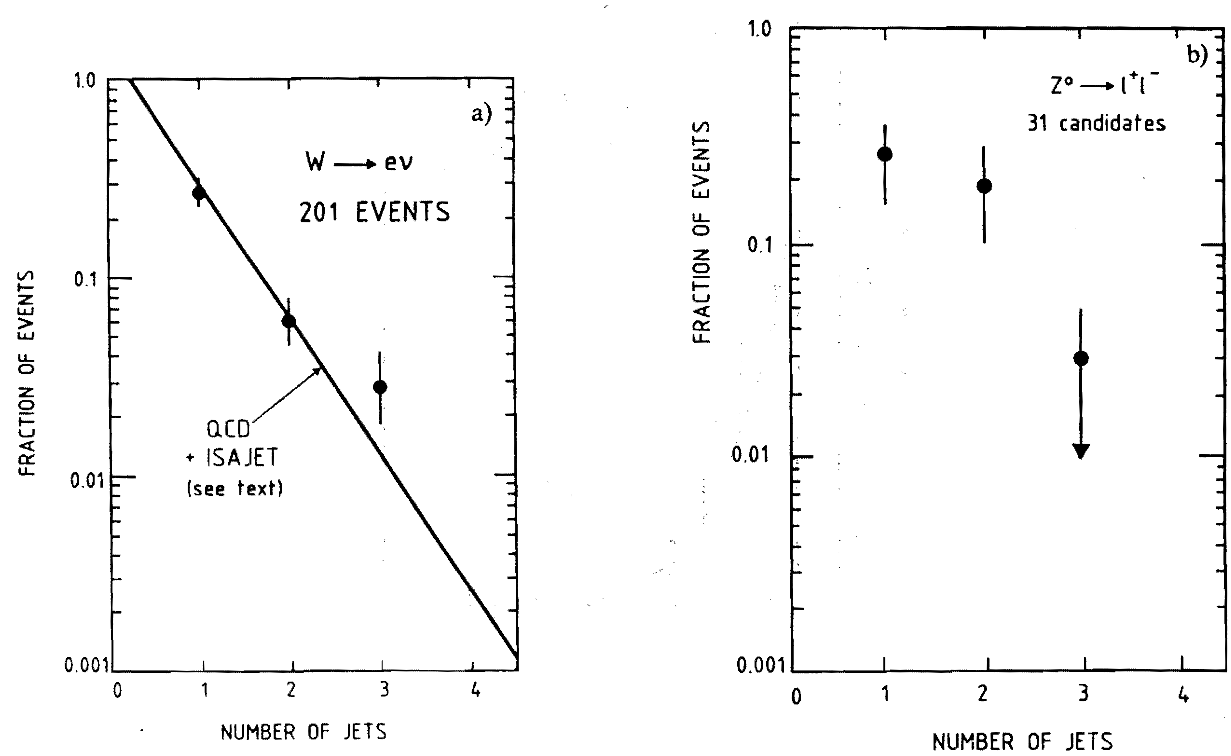

Fig. 10 Jet multiplicity distribution for hadronic jets produced in association with a) W's and b) Z^0's. The QCD curve combines the ISAJET prediction for the rate of (W + 1 jet) events with the assumption that the probability of producing two jets along with the W is equal to the square of the probability to produce one jet. The jet reconstruction efficiency has been taken into account.

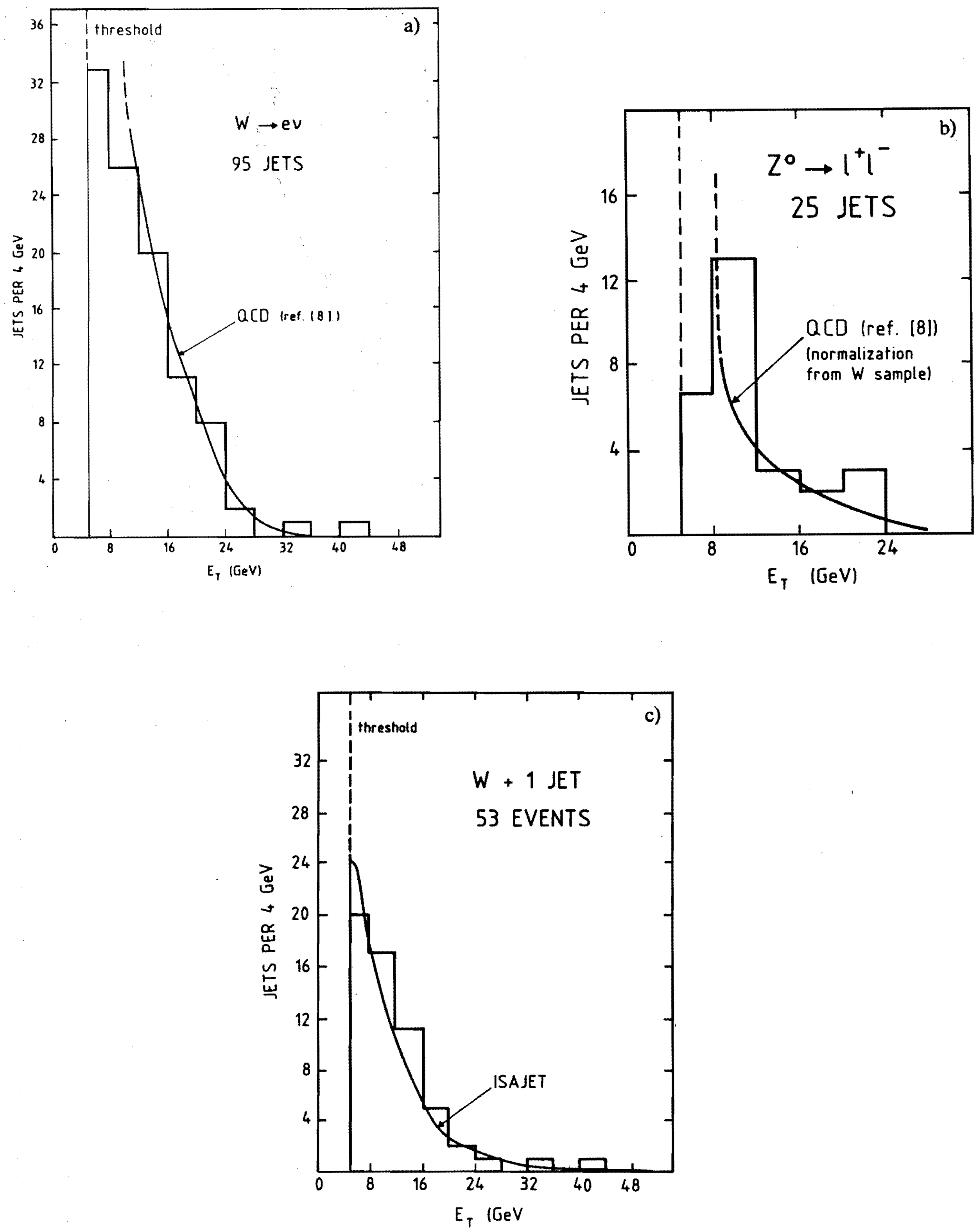

Fig. 11 Jet transverse momentum distribution for a) jets produced in association with W's — the curve shows the QCD prediction of Ref. 8 normalized to the tail of the distribution (the region in which we expect to have good reconstruction efficiency for the jets); b) jets produced in association with Z^0's — the curve shows the same QCD prediction as (a) with the normalization coming from the corresponding normalization used for the W distribution; c) jets produced in W events in which only one hadronic jet is reconstructed — the curve is the ISAJET prediction.

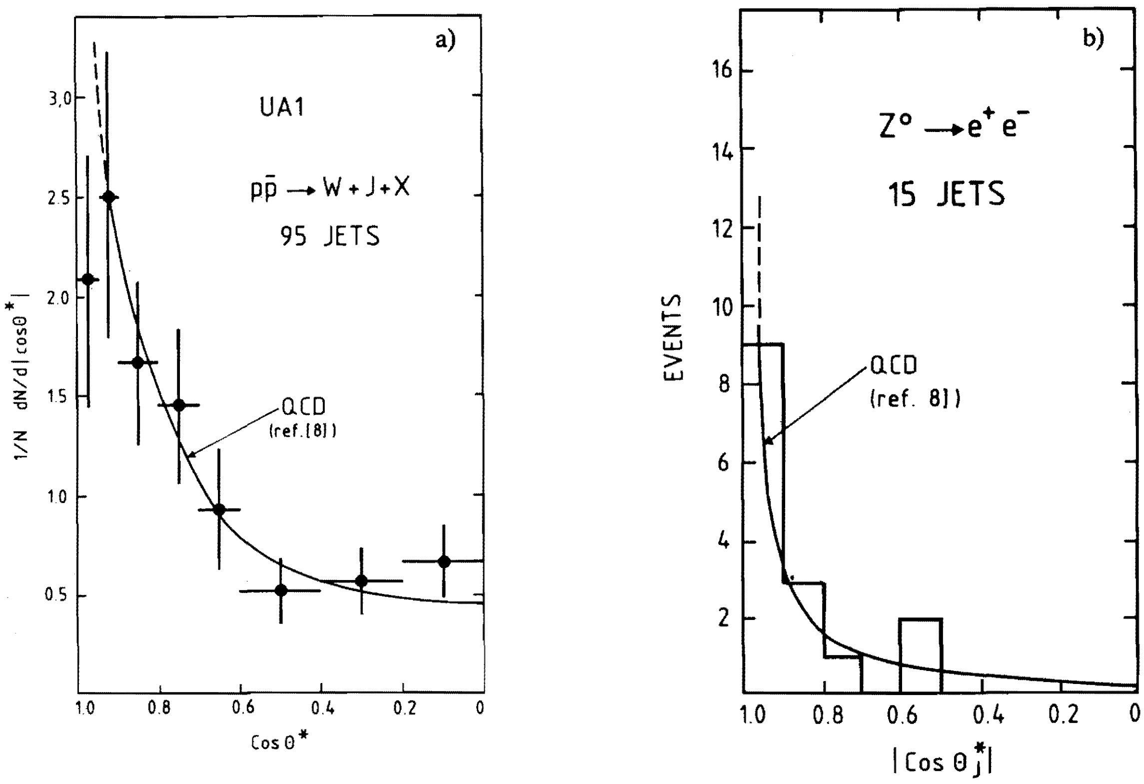

Fig. 12 The angular distribution for jets reconstructed in a) W events and b) Z^0 events is strongly peaked in the beam directions. The distribution of cos θ^* is shown, θ^* being the angle between the jet and the average beam direction in the rest frame of the W and the jet. The curve shows the QCD expectation from Ref. 8.

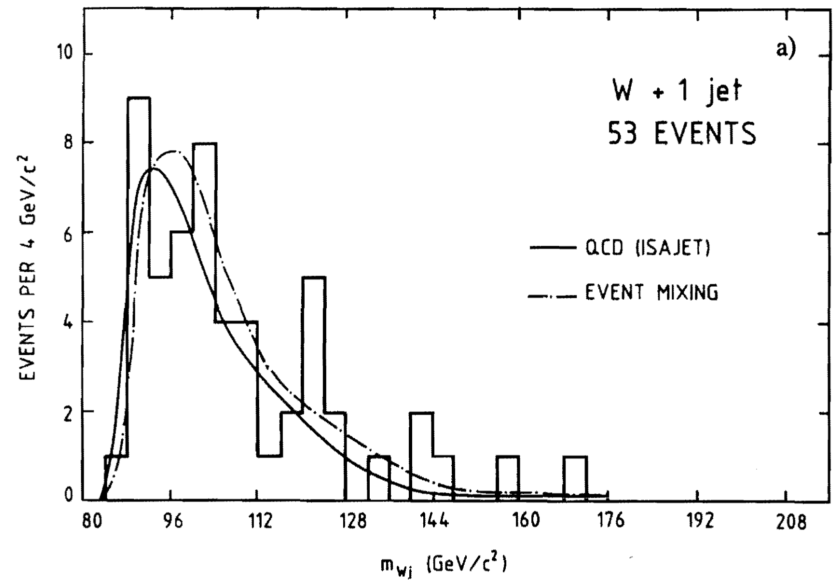

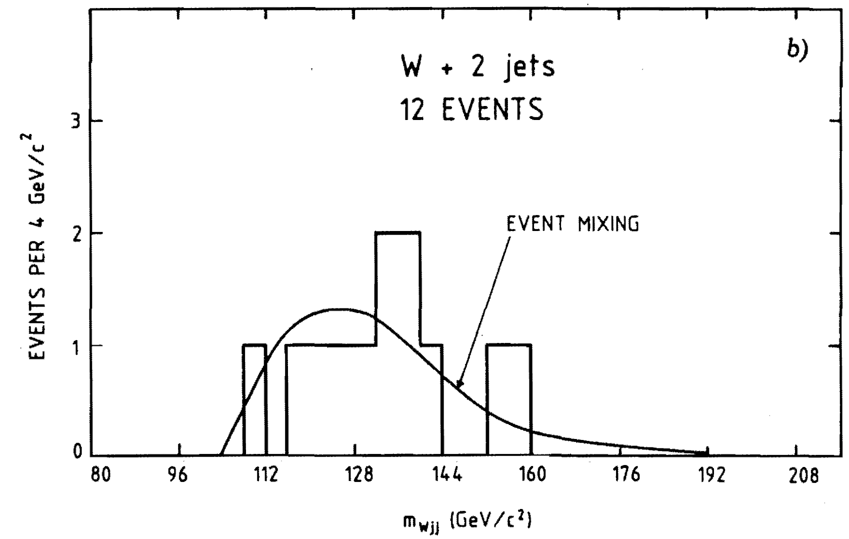

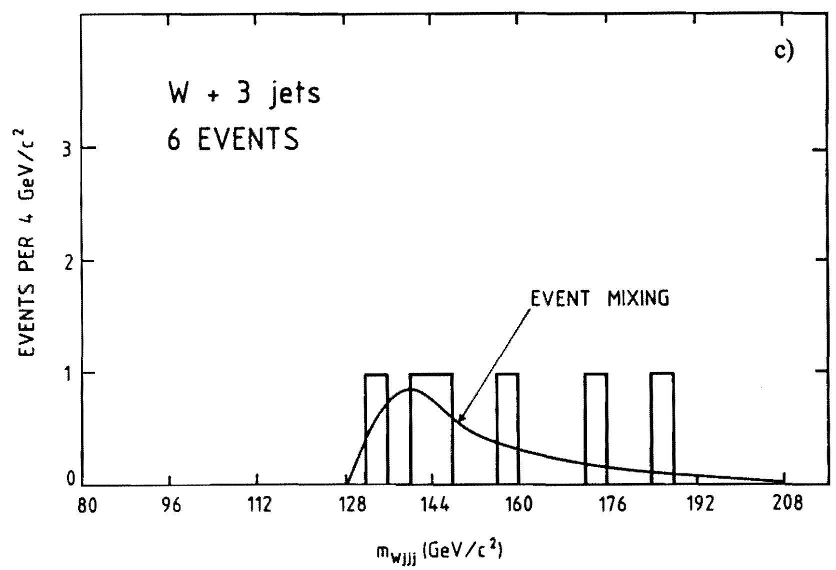

Fig. 13

a) (W + jet) mass distribution. The QCD expectation of ISAJET (solid curve) is shown. The dot-dashed curve shows the expectation from event mixing in which the observed W four-vectors are randomly associated with the four-vectors of hadronic jets observed in W events. b) (W + 2 jet)-mass distribution. The curve shows the expectation from event mixing. c) (W + 3 jet)-mass distribution. The curve shows the expectation from event mixing.

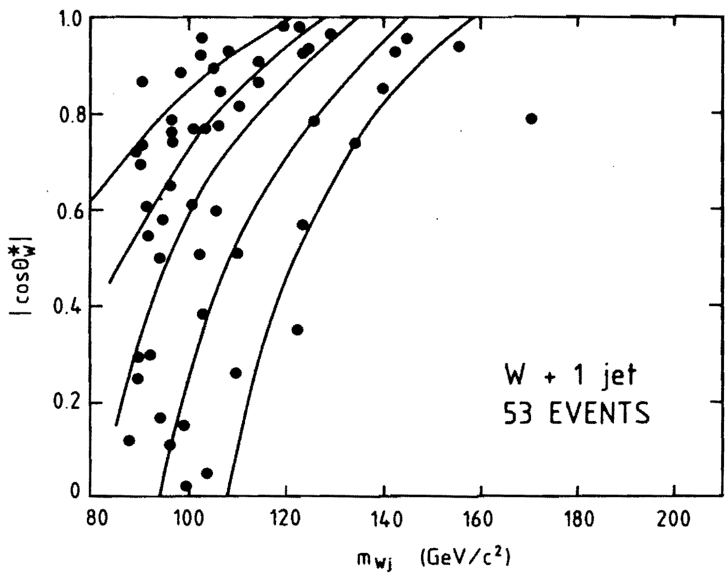

Fig. 14 Two-dimensional plot of cos θ^* versus (W + jet) mass for those W events containing one hadronic jet. The contours show the ISAJET prediction for the population of this plot. In going from right to left, each contour represents an expected doubling in density in the plot.